
Machine Teaching for Inverse Reinforcement Learning: Algorithms and Applications

Daniel S. Brown

Department of Computer Science
University of Texas at Austin
dsbrown@cs.utexas.edu

Scott Niekum

Department of Computer Science
University of Texas at Austin
sniekum@cs.utexas.edu

Abstract

Inverse reinforcement learning (IRL) infers a reward function from demonstrations, allowing for policy improvement and generalization. However, despite much recent interest in IRL, little work has been done to understand of the minimum set of demonstrations needed to teach a specific sequential decision-making task. We formalize the problem of finding optimal demonstrations for IRL as a machine teaching problem where the goal is to find the minimum number of demonstrations needed to specify the reward equivalence class of the demonstrator. We extend previous work on algorithmic teaching for sequential decision-making tasks by showing an equivalence to the set cover problem, and use this equivalence to develop an efficient algorithm for determining the set of maximally-informative demonstrations. We apply our proposed machine teaching algorithm to two novel applications: benchmarking active learning IRL algorithms and developing an IRL algorithm that, rather than assuming demonstrations are i.i.d., uses counterfactual reasoning over informative demonstrations to learn more efficiently.

1 Introduction

As robots and digital personal assistants become more prevalent, there is growing interest in developing algorithms that allow everyday users to program or adapt these intelligent systems to accomplish sequential decision-making tasks, such as performing household chores, or carrying on a meaningful conversation. A common way to teach sequential decision-making tasks is through Learning from Demonstration (LfD) [1], where a human gives demonstrations of desired behavior, and the algorithm attempts to learn a policy based on these demonstrations. More specifically, Inverse Reinforcement Learning (IRL) [2, 3] is a form of LfD that aims to infer the reward function that motivated the demonstrator’s behavior, allowing for reinforcement learning [4] and generalization to unseen states. Despite much recent interest in IRL, there is not a clear, agreed-upon definition of optimality in IRL, namely, what is the minimal set of demonstrations needed to teach a sequential decision-making task.

One popular framework for studying optimal teaching is *machine teaching* [5]. The machine teaching problem is to select the optimal training set that minimizes teaching effort, often defined as the size of the data set, and the loss between the model learned by the student and the learning target. While machine teaching has been applied to regression and classification [6, 7], little work has addressed machine teaching for sequential decision-making tasks such as learning from demonstration via IRL.

The contributions of this paper are threefold: (1) a formal definition of machine teaching for IRL, (2) a novel, efficient algorithm to compute optimal teaching demonstrations for IRL, and (3) two examples of how optimal teaching can be used in practice: benchmarking the performance of active learning IRL algorithms [8, 9, 10] and designing new IRL algorithms that better leverages informative demonstrations that do not follow the i.i.d. assumption made by most IRL algorithms.

2 Related work

Determining the minimum number of demonstrations needed to teach a task falls under the fields of Algorithmic Teaching [11, 12] and Machine Teaching [6, 5]. However, almost all previous work has been limited to optimal teaching for classification and regression tasks. Cakmak and Lopes [13] examined the problem of giving maximally informative demonstrations to teach a sequential decision-making task; however, they do not formally define the optimal solution to the machine teaching problem for IRL and, as we discuss later, their algorithm often underestimates the minimum number of demonstrations needed to teach a task. Other related approaches examine how a robot can give informative demonstrations to a human [14], or formalize optimal teaching as a cooperative two-player Markov game [15]; however, neither approach addresses the machine teaching problem of finding the minimum number of demonstrations needed to teach a task.

In the field of Cognitive Science, researchers have investigated Bayesian models of informative human teaching and the inferences human students make when they know they are being taught [16]. Ho et al. [17] showed that humans give different demonstrations when performing a sequential decision making task, depending on whether they are teaching or simply doing the task. While studies have shown that standard IRL algorithms can benefit from informative demonstrations [13, 17], to the best of our knowledge, no IRL algorithms exist that can explicitly leverage the informative nature of such demonstrations. In Section 7.2 we propose a novel IRL algorithm that can learn more efficiently from informative demonstrations than standard IRL algorithms which assume i.i.d. demonstrations.

3 Problem formalism

3.1 Markov decision processes

We model the environment as a Markov decision process (MDP), $\langle S, \mathcal{A}, T, R, \gamma, S_0 \rangle$, where S is the set of states, \mathcal{A} is the set of actions, $T : S \times \mathcal{A} \times S \rightarrow [0, 1]$ is the transition function, $R : S \rightarrow \mathbb{R}$ is the reward function, $\gamma \in [0, 1)$ is the discount factor, and S_0 is the initial state distribution. A policy $\pi : S \times \mathcal{A} \mapsto [0, 1]$ is a mapping from states to a probability distribution over actions. The value of executing policy π starting at state $s \in S$ is defined as $V^\pi(s) = \mathbb{E}[\sum_{t=0}^{\infty} \gamma^t R(s_t) | \pi, s_0 = s]$. The Q-value of a state-action pair (s, a) is defined as $Q^\pi(s, a) = R(s) + \gamma \mathbb{E}_{s' \sim T(\cdot | s, a)} [V^\pi(s')]$. We denote the optimal Q-value functions as $Q^*(s, a) = \max_\pi Q^\pi(s, a)$.

As is common in the literature [18, 19, 20], we assume that the reward function can be expressed as a linear combination of features, $\phi : S \mapsto \mathbb{R}^k$, so that $R(s) = \mathbf{w}^T \phi(s)$ where $\mathbf{w} \in \mathbb{R}^k$ is the vector of feature weights. Given this assumption, we can write the expected discounted return of a policy as $\rho(\pi) = \mathbb{E}[\sum_{t=0}^{\infty} \gamma^t \mathbf{w}^T \phi(s_t) | \pi] = \mathbf{w}^T \mu_\pi$, where $\mu_\pi = \mathbb{E}[\sum_{t=0}^{\infty} \gamma^t \phi(s_t) | \pi]$.

3.2 Machine teaching

The machine teaching problem [6] is to select the optimal training set D^* that minimizes the teaching effort, often defined as the size of the data set, and the loss between the model learned by the student and the learning target θ^* . The optimization problem for machine teaching can be written as $\min_D \text{loss}(\hat{\theta}_D, \theta^*) + \text{effort}(D)$, where D is the training set, $\hat{\theta}_D$ is the model the student learns under D , and θ^* is the model the teacher desires the student to learn.

3.3 Problem definition

We now formulate the optimal teaching problem for IRL as a machine teaching problem [5]. We assume that the expert teacher has a true reward R^* and is able to demonstrate state-action pairs (s, a) by executing the corresponding optimal policy π^* . The machine teaching problem for IRL could be stated as determining the minimal set of demonstrations, \mathcal{D} , that enables an IRL agent to learn R^* . However, IRL is ill-posed [2]—there are an infinite number of reward functions that explain any optimal policy. Instead, we focus on determining the minimal set of demonstrations that enable an learner to find a reward function that is behaviorally equivalent to π^* . We define the *behavior equivalence class* (BEC) of a policy π as the set of reward functions under which π is optimal:

$$\text{BEC}(\pi) = \{\mathbf{w} \in \mathbb{R}^k \mid \pi \text{ is optimal under } R(s) = \mathbf{w}^T \phi(s)\}. \quad (1)$$

We now formalize the machine teaching problem for IRL.

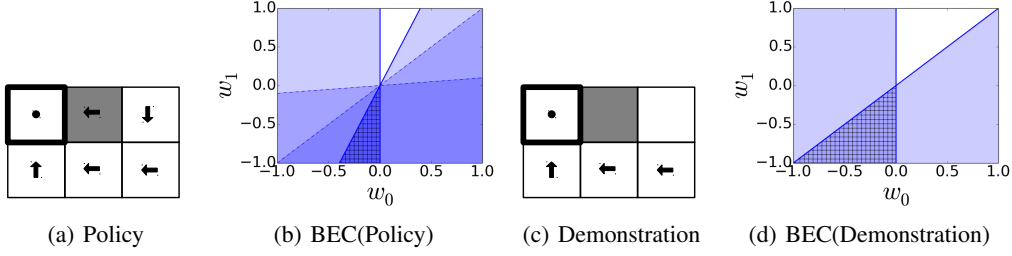


Figure 1: Behavioral equivalence classes (BEC) for a simple grid world with 6 states. The upper left state is a terminal state. Each state has 4 available actions and the reward function is a linear combination of two binary features that indicate whether the color of the cell is white or grey. (a) Arrows show the optimal policy for this grid world. (b) The resulting intersection of halfspaces (shaded region) that defines all weight vectors such that the policy shown in (a) is optimal. (c) Demonstration from the optimal policy in (a). (d) Intersection of halfspaces (shaded region) resulting from the demonstration.

Machine teaching problem for IRL: Given an MDP, $\mathcal{M} = \langle \mathcal{S}, \mathcal{A}, T, R^*, S_0, \gamma \rangle$ and optimal policy π^* , find the set of demonstrations, \mathcal{D} , that the minimises the following optimization problem:

$$\min_{\mathcal{D}} \text{loss}(\hat{R}_{\mathcal{D}}, \pi^*) + \text{effort}(\mathcal{D}) \quad (2)$$

where R^* is the teacher’s true reward, $\hat{R}_{\mathcal{D}}$ is the reward recovered by the learner using IRL,

$$\text{loss}(\hat{R}_{\mathcal{D}}, \pi^*) = \begin{cases} 0 & \text{if } \hat{R}_{\mathcal{D}} \in \text{BEC}(\pi^*), \\ \infty & \text{otherwise,} \end{cases} \quad (3)$$

and, unless specified otherwise, $\text{effort}(\mathcal{D}) = |\mathcal{D}|$, the number of (s, a) pairs in \mathcal{D} .

4 Characterizing behavioral equivalence classes

Given a formal definition of machine teaching for IRL, we now briefly discuss how to calculate the behavioral equivalence class for both a policy and for a set of demonstrations from a policy. Given an MDP with either finite or continuous states, with a reward function represented as a linear combination of features, Ng and Russell [2] derived the behavioral equivalence class (BEC) for a policy. We summarize their result in the following theorem:

Theorem 1. [2] *Given an MDP, $\text{BEC}(\pi)$ is given by the following intersection of halfspaces:*

$$\mathbf{w}^T (\mu_{\pi}^{(s,a)} - \mu_{\pi}^{(s,b)}) \geq 0, \quad \forall a \in \arg \max_{a' \in \mathcal{A}} Q^*(s, a'), b \in \mathcal{A}, s \in \mathcal{S}, \quad (4)$$

where $\mathbf{w} \in \mathbb{R}^k$ are the reward function weights and $\mu_{\pi}^{(s,a)} = \mathbb{E}[\sum_{t=0}^{\infty} \gamma^t \phi(s_t) | \pi, s_0 = s, a_0 = a]$, is the vector of expected feature counts from taking action a in state s and acting optimally thereafter.

We can define the BEC for a set of demonstrations \mathcal{D} from a policy π similarly:

Corollary 1. *$\text{BEC}(\mathcal{D} | \pi)$ is given by the following intersection of halfspaces:*

$$\mathbf{w}^T (\mu_{\pi}(s, a) - \mu_{\pi}(s, b)) \geq 0, \quad \forall (s, a) \in \mathcal{D}, b \in \mathcal{A}. \quad (5)$$

All proofs can be found in the Supplement.

Example: Consider the grid world shown in Figure 1(a), with four actions available in each state and deterministic transitions. We computed the BEC using a featurized reward function $R(s) = \mathbf{w}^T \phi(s)$, where $\mathbf{w} = (w_0, w_1)$ is the binary feature weight vector with w_0 indicating “white” and w_1 indicating “grey” (see the Supplement for full details). The resulting halfspace constraints are shown in Figure 1(b). The intersection of these halfspaces exactly describes the set of rewards that make the policy shown in Figure 1(a) optimal: both white and grey cells have negative reward and the weight for the grey feature is low enough that the optimal policy avoids the shaded cell.

Figures 1(c) and 1(d) show the BEC of a demonstration. The demonstration shows that both features are non-positive and that w_1 is no better than w_0 (otherwise the demonstration would have gone through the grey region); however, the demonstration leaves open the possibility that all feature weights are equal. However, if the demonstration had started in the top right cell, the BEC of the demonstration would equal the BEC of the optimal policy. This highlights the fact that some demonstrations are more informative than others. An efficient algorithm for finding maximally informative demonstrations is one of the contributions of this paper.

5 Prior work on algorithmic teaching of sequential decision-making tasks

We now give an overview of the algorithm proposed by Cakmak and Lopes [13] which is most related to our work. The main insight that Cakmak and Lopes use is that of Corollary 2: if a demonstration from π^* contains (s, a) , then $Q^*(s, a) \geq Q^*(s, b) \iff \mathbf{w}^T(\mu_\pi^{(s,a)} - \mu_\pi^{(s,b)}) \geq 0, \forall b \in \mathcal{A}$.

Given a demonstration set \mathcal{D} , Cakmak and Lopes use the intersection of the corresponding halfspaces (as defined in Corollary 2) as a representation of the learner’s uncertainty over the true reward function. They use a Monte Carlo estimate of the volume of this cone as a measure of the learner’s uncertainty, and seek demonstrations that minimize the uncertainty, $G(\mathcal{D})$, over the true reward function, where

$$G(\mathcal{D}) = \frac{1}{N} \sum_{j=1}^N \delta(x_j \in C(\mathcal{D})), \quad (6)$$

δ is an indicator function, $C(\mathcal{D})$ is the intersection of halfspaces given in Corollary 2, and the volume is estimated by drawing N random points x_j from $[-1, 1]^k$. The set of maximally informative demonstrations is chosen greedily by iterating over the initial states and selecting the trajectory that maximally decreases $G(\mathcal{D})$. This process repeats until $G(\mathcal{D})$ falls below a user defined threshold ϵ . We refer to this algorithm as the Uncertainty Volume Minimization (UVM) algorithm.

In the UVM Algorithm, trajectories are added until $G(\mathcal{D})$ is below some user-provided threshold ϵ . However, this threshold must be carefully tuned for each MDP. If ϵ is too low, then the algorithm will never terminate. Alternatively, if ϵ is too high, then not enough demonstrations will be selected to teach an appropriate reward function. In our experiments we remove the need for parameter tuning by stopping the algorithm if it cannot add another demonstration that decreases $G(\mathcal{D})$.

The main limitation of the UVM algorithm is that of volume estimation—exact volume estimation is $\#P$ -hard [21, 22] and straightforward Monte Carlo estimation is known to fail in high-dimensions [22]. Additionally, if there are two (or more) actions that are both optimal in a given state s , and those two actions (call them a and b) are demonstrated, this results in the following halfspace constraints:

$$w^T(\mu_\pi^{(s,a)} - \mu_\pi^{(s,b)}) \geq 0 \text{ and } w^T(\mu_\pi^{(s,b)} - \mu_\pi^{(s,a)}) \geq 0 \Rightarrow w^T(\mu_\pi^{(s,b)} - \mu_\pi^{(s,a)}) = 0 \quad (7)$$

This is problematic since any strict subspace of \mathbb{R}^k has measure zero, resulting in an uncertainty volume of zero. Thus, for any optimal policy where there exists a state with two or more optimal actions, the UVM algorithm will terminate with zero uncertainty if these two optimal actions are added to \mathcal{D} , even if this leaves an entire $(k - 1)$ dimensional subspace of uncertainty over the reward. One solution would be to use more sophisticated sampling techniques such as hit-and-run sampling [23]. However, these methods still assume there are points on the interior of the sampling region and can be computationally intensive as they still require running long Markov chains to ensure good mixing. We instead propose a novel approach based on a set cover equivalence.

6 Set cover optimal teaching for IRL

Our proposed algorithm seeks to remedy the problems with the UVM algorithm identified in the previous section. Our first insight is that because the behavioral equivalence class for π^* is an intersection of halfspaces (Theorem 3), rather than give demonstrations until the uncertainty volume, $G(\mathcal{D})$, is less than some arbitrary ϵ , demonstrations should be chosen specifically to define $\text{BEC}(\pi^*)$. Thus, a solution to the optimal teaching problem for IRL should select the demonstration set \mathcal{D} such that $|\mathcal{D}|$ is minimized and the corresponding intersection of halfspaces is equal to $\text{BEC}(\pi^*)$.

Our second insight is to formulate an efficient approximation algorithm for the IRL machine teaching problem through an equivalence to the set cover problem. This allows us to transform a difficult

Table 1: Comparison of Uncertainty Volume Minimization (UVM) and Set Cover Optimal Teaching (SCOT) averaged across 20 random 9x9 grid worlds with 8-dimensional features. UVM(x) was run using x Monte Carlo samples. UVM underestimates the number of (s, a) pairs needed to teach π^* .

	Ave. number of (s, a) pairs	Ave. % incorrect actions	Ave. time (s)
UVM (10^5)	5.150	31.420	567.961
UVM (10^6)	6.650	19.568	1620.578
UVM (10^7)	8.450	18.642	10291.365
SCOT	16.200	0.679	0.901

volume estimation problem into a well known discrete optimization problem. From Section 4 we know that the behavioral equivalence class of both a policy and a demonstration are both characterized by intersections of halfspaces, and each demonstration from π^* produces an intersection of halfspaces which contains $\text{BEC}(\pi^*)$. Thus, the Machine Teaching Problem for IRL (Section 3.3) is an instance of the set cover problem: we have a set of halfspaces defining $\text{BEC}(\pi^*)$, each possible trajectory from π^* covers zero or more of the halfspaces that define $\text{BEC}(\pi^*)$, and we wish to find the smallest set of demonstrations, \mathcal{D} , such that $\text{BEC}(\mathcal{D}|\pi^*) = \text{BEC}(\pi^*)$.

One potential issue is that, as seen in Figure 1, many halfspace constraints will be non-binding and we are only interested in covering the non-redundant halfspace constraints that minimally define $\text{BEC}(\pi^*)$. To address this, we use linear programming to efficiently remove redundant halfspaces before running our set cover algorithm (see the Supplement for specific details).

Our algorithm is as follows: (1) find the halfspace constraints for π^* using Theorem 3, (2) find the minimal representation of $\text{BEC}(\pi^*)$ using linear programming, (3) use π^* to compute m trajectories of length H from each starting state and their corresponding halfspace normal vectors using Corollary 2, (4) greedily cover all halfspaces in $\text{BEC}(\pi^*)$ by sequentially picking the trajectory that covers the most uncovered halfspaces. We call this algorithm the Set Cover Optimal Teaching (SCOT).

Whereas UVM finds demonstrations that successively slice off volume until the uncertainty region cannot be reduced, SCOT directly finds the necessary demonstrations that exactly constrain $\text{BEC}(\pi^*)$. This removes the both the need to calculate high-dimensional volumes and the need to determine an appropriate stopping threshold. SCOT also has the following properties:

Proposition 1. *The Set Cover Optimal Teaching (SCOT) algorithm always terminates.*

Theorem 2. *Under the assumption of error-free demonstrations, SCOT is a $(1 - 1/e)$ -approximation to the Machine Teaching Problem for IRL (Section 3.3) for the following learning algorithms: Bayesian IRL [24, 25], Policy Matching [26], and Maximum Likelihood IRL [27, 8].*

6.1 Algorithm comparison

To compare the performance of SCOT and UVM, we ran an experiment on random 9x9 grid worlds with 8-dimensional one-hot binary features per cell. We computed maximally informative demonstration sets with SCOT and UVM using trajectories consisting of single state-action pairs. We measured the performance loss for each algorithm by running IRL to find the maximum likelihood reward function given the demonstrations and then calculating the percentage of states where the resulting policy took a suboptimal action under the true reward. Table 2 shows that the UVM algorithm underestimates the size of the optimal teaching set of demonstrations, due to the difficulty of estimating volumes as discussed earlier, resulting in high performance loss. We tried sampling more points, but found that this only slightly improved performance loss while significantly increasing run-time. Compared to UVM, SCOT successfully finds good demonstrations that lead to the correct behavior equivalence class, with orders of magnitude less computation.

To further explore the sensitivity of UVM to the number of features, we ran a test on a fixed size grid world with varying numbers of features. We used a deterministic policy to ameliorate the problems with volume computation discussed in Section 5. We found that SCOT is robust for high-dimensional feature spaces, whereas UVM consistently underestimates the minimum number of demonstrations needed when there are 10 or more features, even when teaching a deterministic policy (see Supplement for details).

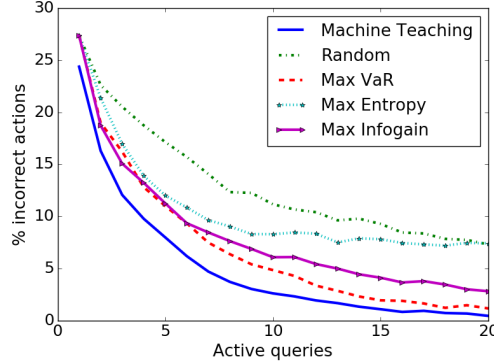


Figure 2: Performance of different active IRL algorithms compared to an approximately optimal machine teaching benchmark. Results are averaged over 100 random 10x10 grid worlds.

7 Applications of machine teaching for IRL

7.1 Benchmarking active IRL algorithms

Our first application is to provide a performance bound for active IRL algorithms [8, 9, 10]. The SCOT algorithm requires knowledge of the optimal policy, so it cannot be used directly as an active learning algorithm. Instead, we use SCOT as a tractable approximation to the optimal sequence of queries for an active learning IRL agent, allowing us to benchmark different active IRL algorithms.

We evaluated two active query strategies from the literature: *Max Entropy*, a strategy proposed by Lopes et al. [8] that queries the state with the highest action entropy and *Max Infogain*, a strategy proposed by Cui et al. [10] that selects the trajectory with the largest expected change in the posterior $P(R|D)$. We also propose a novel active IRL strategy, *Max VaR*, inspired by recent work on risk-aware IRL [28]. *Max VaR* queries the optimal action at the state where the maximum likelihood action given the current demonstrations has the highest 0.95-Value-at-Risk (95th-percentile policy loss over the posterior) [28, 29]. We compare these algorithms with random queries and to the approximately maximally informative sequence of queries found using SCOT.

We ran an experiment on 100 random 10x10 grid worlds with 10-dimensional binary one-hot features. Figure 2 shows the performance loss for each active IRL algorithm. Each iteration corresponds to a single state query and a corresponding optimal trajectory from that state. After adding each new trajectory to \mathcal{D} , the MAP reward function is found using Bayesian IRL[24], and the corresponding optimal policy is compared against the optimal policy under the true reward function.

The results in Figure 2 show that all active IRL approaches do well for early queries, but that Max Entropy ends up performing no better than random as the number of queries increases. This result matches the findings of prior work which showed that active entropy queries perform similarly to random queries for complex domains [8, 9]. Max VaR and Max Infogain perform better than Max Entropy for later queries. By benchmarking the performance of Max VaR and Max Infogain against SCOT we see that the machine teaching benchmark shows that Max VaR is a close approximation to the maximally informative sequence of queries, without requiring knowledge of the optimal policy.

7.2 Using optimal teaching to improve IRL

For our second application, we explore using machine teaching as a novel way to improve IRL. Human teachers are known to give highly informative, non i.i.d. demonstrations when teaching [17, 16]. For example, when giving demonstrations, human teachers do not randomly sample from the optimal policy, potentially giving the same (or highly similar) demonstration twice. However, existing IRL approaches usually assume demonstrations are drawn, i.i.d. from the demonstrator’s policy [24, 18, 27, 30]. We propose to add a notion of information optimality to Bayesian IRL (BIRL) [24]. We call our algorithm Bayesian Information-Optimal IRL or BIO-IRL. The main idea is that if the learner knows a teacher is giving informative demonstrations, then the learner should select a reward function that makes the demonstrations look both optimal and informative.

7.2.1 BIO-IRL algorithm

Our proposed algorithm allows the assumption of an expert teacher: demonstrations not only follow π^* , but are also highly informative. We use the following likelihood for BIO-IRL:

$$P(D|R) \propto P_{\text{info}}(\mathcal{D}|R) \cdot \prod_{(s,a) \in \mathcal{D}} P((s,a)|R) \quad (8)$$

where $P((s,a)|R)$ is the standard softmax likelihood from BIRL [24] that measures the likelihood of taking action a in state s under R , while $P_{\text{info}}(\mathcal{D}|R)$ measures how informative the entire demonstration set \mathcal{D} appears under R .

We compute $P_{\text{info}}(\mathcal{D}|R)$ as follows. Given a demonstration set \mathcal{D} and a hypothesis reward function R , we first compute the information gap, $\text{infoGap}(\mathcal{D}, R)$, which uses behavioral equivalence classes to compare the relative informativeness of \mathcal{D} under R , with the informativeness of the maximally informative teaching set \mathcal{D}^* under R (see Algorithm 1). We estimate informativeness by computing the angular similarity between halfspace normal vectors as detailed in the Supplement. BIO-IRL uses the absolute difference between angular similarities to counterfactually reason about the gap in informativeness between the actual demonstration and an equally sized machine teaching demonstration. Given the actual demonstration \mathcal{D} and the machine teaching demonstration \mathcal{D}^* under R , we let

$$P_{\text{info}}(\mathcal{D}|R) \propto \exp(-\lambda \cdot \text{infoGap}(\mathcal{D}, R)) \quad (9)$$

where λ is a hyperparameter modeling the confidence that the demonstrations are informative. If $\lambda = 0$, then BIO-IRL is equivalent to standard BIRL.

Algorithm 1 $\text{infoGap}(\mathcal{D}, R)$

- 1: Calculate π^* under R
 - 2: Calculate $\text{BEC}(\pi^*)$, $\text{BEC}(\mathcal{D}|\pi^*)$
 - 3: $\mathcal{D}^* \leftarrow \text{SCOT}(\pi^*)$
 - 4: $m \leftarrow$ number of trajectories in \mathcal{D}
 - 5: $\mathcal{D}_{1:m}^* \leftarrow$ first m trajectories in \mathcal{D}^*
 - 6: Calculate $\text{BEC}(\mathcal{D}^*|\pi^*)$
 - 7: $\text{infoDemo} \leftarrow \text{angularSim}(\text{BEC}(\mathcal{D}|\pi^*), \text{BEC}(\pi^*))$
 - 8: $\text{infoCounterfactual} \leftarrow \text{angularSim}(\text{BEC}(\mathcal{D}_{1:m}^*|\pi^*), \text{BEC}(\pi^*))$
 - 9: **return** $\text{abs}(\text{infoDemo} - \text{infoCounterfactual})$
-

7.2.2 Experiments

Consider the Markov chain in Figure 3. If an information-optimal demonstrator gives the demonstration shown on the left, BIO-IRL assumes that both the orange and black features are equally preferable over white. This is because, given different preferences, an informative teacher would have given a different demonstration. For example, if the black feature was always preferred over white and orange, a maximally informative demonstration would have started in the leftmost state and moved right until it reached the rightmost state. Because the likelihood function for standard BIRL only measures how well the demonstration matches the optimal policy for a given reward function, BIRL assigns equal likelihoods to all reward functions that result in one of the policy candidates shown in the center of the Figure 3. The bar graph in Figure 3 shows the likelihood of each policy candidate under BIRL and BIO-IRL with different λ parameters. Rather than assigning equal likelihoods, BIO-IRL puts higher likelihood on Policy A, the policy that makes the demonstration appear maximally informative. Changing the likelihood function to reflect informative demonstrations results in a tighter posterior distribution over likely rewards, which is important if the agent wants to reason about the safety of its learned policy given limited demonstrations [31].

We also evaluated BIO-IRL in a simulated ball sorting task shown in Figure 4(a). In this task, balls start in one of 36 evenly spaced starting conditions and need to be moved into one of four bins located on the corners of the table. Demonstrations are given by selecting an initial state for the ball and moving the ball until it is in one of the bins. Actions are discretized to the four cardinal directions along the table top and the reward is a linear combination of five indicator features representing whether the ball is in one of the four bins or on the table. We generated 50 random rewards and used a discount factor of $\gamma = 0.95$, this allows for a wide variety of preferences over bin placement which

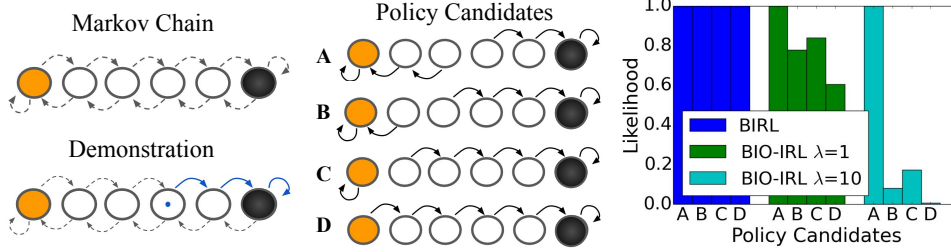


Figure 3: Simple Markov chain with three features (orange, white, black) and two actions available in each state. Left: demonstration in blue. Center: all policies that are consistent with the demonstration. Right: likelihoods for BIRL and BIO-IRL with $\lambda = 1$ and 10. BIRL gives all rewards that lead to any of the policy candidates a likelihood of 1.0 since it only reasons about the optimality of the demonstration under a hypothesis reward. BIO-IRL reasons about both the optimality of the demonstration and the informativeness of the demonstration and gives highest likelihood to rewards that make policy A optimal.

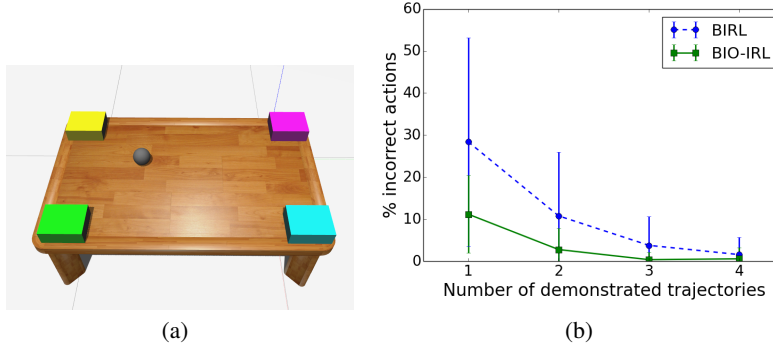


Figure 4: (a) Ball sorting task. The ball starts at one of 36 positions on the table and must be moved into one of four bins depending on the demonstrator’s preferences. (b) Comparison of MAP policies found by BIO-IRL and BIRL when receiving maximally informative demonstrations.

can depend on the distance of the ball to the different bins. For each reward function, informative trajectories were generated using SCOT and given sequentially to BIRL and BIO-IRL. Figure 4(b) shows that BIO-IRL learns more efficiently than BIRL, often learning the optimal policy after only two demonstrations (see the Supplement for full details).

8 Conclusion and future work

We formalized the Machine Teaching Problem for IRL and proposed an approximate set cover-based solution to this problem. Our proposed approach enables an efficient and robust algorithm for selecting maximally informative demonstrations that shows several orders of magnitude improvement in computation time over prior work and is robust to high-dimensional feature spaces. We applied our machine teaching algorithm to two novel applications: benchmarking active learning algorithms and improving the efficiency of IRL when receiving informative demonstrations. Benchmarking active IRL against an approximately optimal query strategy shows that recent approaches, including a novel risk-sensitive approach, are approaching the machine teaching lower bound on sample complexity. For our second application, we demonstrated that when being taught by an expert teacher, IRL algorithms that can model the informativeness of demonstrations learn more efficiently than simply assuming i.i.d. demonstrations. Future work includes applying and extending our proposed machine teaching framework to quantify the inherent difficulty of teaching common IRL benchmark tasks, to improve how robots convey their objectives to humans [14], to help robots better learn from noisy but informative human demonstrations, and to study optimal training set attacks [32, 33] in the context of IRL in order to design algorithms that are robust to incidental noise and poor demonstrations.

References

- [1] Brenna D. Argall, Sonia Chernova, Manuela Veloso, and Brett Browning. A survey of robot learning from demonstration. *Robotics and Autonomous Systems*, 57(5):469–483, 2009.
- [2] Andrew Y Ng and Stuart J Russell. Algorithms for inverse reinforcement learning. In *ICML*, pages 663–670, 2000.
- [3] Pieter Abbeel and Andrew Y Ng. Apprenticeship learning via inverse reinforcement learning. In *Proceedings of the twenty-first international conference on Machine learning*, page 1. ACM, 2004.
- [4] Richard S Sutton and Andrew G Barto. *Reinforcement learning: An introduction*, volume 1. MIT press Cambridge, 1998.
- [5] Xiaojin Zhu. Machine teaching: An inverse problem to machine learning and an approach toward optimal education. In *AAAI*, pages 4083–4087, 2015.
- [6] Xiaojin Zhu. Machine teaching for bayesian learners in the exponential family. In *Advances in Neural Information Processing Systems*, pages 1905–1913, 2013.
- [7] Ji Liu and Xiaojin Zhu. The teaching dimension of linear learners. *Journal of Machine Learning Research*, 17(162):1–25, 2016.
- [8] Manuel Lopes, Francisco Melo, and Luis Montesano. Active learning for reward estimation in inverse reinforcement learning. In *Joint European Conference on Machine Learning and Knowledge Discovery in Databases*, pages 31–46. Springer, 2009.
- [9] Robert Cohn, Edmund Durfee, and Satinder Singh. Comparing action-query strategies in semi-autonomous agents. In *The 10th International Conference on Autonomous Agents and Multiagent Systems-Volume 3*, pages 1287–1288. International Foundation for Autonomous Agents and Multiagent Systems, 2011.
- [10] Yuchen Cui and Scott Niekum. Active learning from critiques via bayesian inverse reinforcement learning. In *Robotics: Science and Systems Workshop on Mathematical Models, Algorithms, and Human-Robot Interaction*, 2017.
- [11] Sally A Goldman and Michael J Kearns. On the complexity of teaching. *Journal of Computer and System Sciences*, 50(1):20–31, 1995.
- [12] Frank J Balbach and Thomas Zeugmann. Recent developments in algorithmic teaching. In *International Conference on Language and Automata Theory and Applications*, pages 1–18. Springer, 2009.
- [13] Maya Cakmak and Manuel Lopes. Algorithmic and human teaching of sequential decision tasks. In *AAAI*, 2012.
- [14] Sandy H Huang, David Held, Pieter Abbeel, and Anca D Dragan. Enabling robots to communicate their objectives. In *Robotics: Science and Systems*, 2017.
- [15] Dylan Hadfield-Menell, Stuart J Russell, Pieter Abbeel, and Anca Dragan. Cooperative inverse reinforcement learning. In D. D. Lee, M. Sugiyama, U. V. Luxburg, I. Guyon, and R. Garnett, editors, *Advances in Neural Information Processing Systems 29*, pages 3909–3917. Curran Associates, Inc., 2016.
- [16] Patrick Shafto and Noah Goodman. Teaching games: Statistical sampling assumptions for learning in pedagogical situations.
- [17] Mark K Ho, Michael Littman, James MacGlashan, Fiery Cushman, and Joseph L Austerweil. Showing versus doing: Teaching by demonstration. In *Advances In Neural Information Processing Systems*, pages 3027–3035, 2016.
- [18] Brian D Ziebart, Andrew L Maas, J Andrew Bagnell, and Anind K Dey. Maximum entropy inverse reinforcement learning. In *AAAI*, pages 1433–1438, 2008.
- [19] Dorsa Sadigh, S Shankar Sastry, Sanjit A Seshia, and Anca Dragan. Information gathering actions over human internal state. In *Intelligent Robots and Systems (IROS), 2016 IEEE/RSJ International Conference on*, pages 66–73. IEEE, 2016.
- [20] Matteo Pirotta and Marcello Restelli. Inverse reinforcement learning through policy gradient minimization. In *AAAI*, pages 1993–1999, 2016.
- [21] Leslie G Valiant. The complexity of computing the permanent. *Theoretical computer science*, 8(2):189–201, 1979.
- [22] Miklós Simonovits. How to compute the volume in high dimension? *Mathematical programming*, 97(1):337–374, 2003.
- [23] Robert L Smith. Efficient monte carlo procedures for generating points uniformly distributed over bounded regions. *Operations Research*, 32(6):1296–1308, 1984.
- [24] Deepak Ramachandran and Eyal Amir. Bayesian inverse reinforcement learning. In *Proceedings of the 20th International Joint Conference on Artificial intelligence*, pages 2586–2591, 2007.

- [25] Jaedeug Choi and Kee-Eung Kim. Map inference for bayesian inverse reinforcement learning. In *Advances in Neural Information Processing Systems*, pages 1989–1997, 2011.
- [26] Gergely Neu and Csaba Szepesvári. Apprenticeship learning using inverse reinforcement learning and gradient methods. In *Proc. of 23rd Conference Annual Conference on Uncertainty in Artificial Intelligence*, pages 295–302, 2007.
- [27] Monica Babes, Vukosi Marivate, Kaushik Subramanian, and Michael L Littman. Apprenticeship learning about multiple intentions. In *Proceedings of the 28th International Conference on Machine Learning (ICML-11)*, pages 897–904, 2011.
- [28] Daniel S. Brown and Scott Niekum. Efficient Probabilistic Performance Bounds for Inverse Reinforcement Learning. In *AAAI Conference on Artificial Intelligence*, 2018.
- [29] Philippe Jorion. *Value at risk*. McGraw-Hill, New York, 1997.
- [30] Justin Fu, Katie Luo, and Sergey Levine. Learning robust rewards with adversarial inverse reinforcement learning. *arXiv preprint arXiv:1710.11248*, 2017.
- [31] Daniel S. Brown and Scott Niekum. Toward probabilistic safety bounds for robot learning from demonstration. In *AAAI Fall Symposium on AI for HRI*, 2017.
- [32] Shike Mei and Xiaojin Zhu. Using machine teaching to identify optimal training-set attacks on machine learners. In *AAAI*, pages 2871–2877, 2015.
- [33] Scott Alfeld, Xiaojin Zhu, and Paul Barford. Explicit defense actions against test-set attacks. In *AAAI*, pages 1274–1280, 2017.
- [34] Laurence A Wolsey. An analysis of the greedy algorithm for the submodular set covering problem. *Combinatorica*, 2(4):385–393, 1982.
- [35] George L Nemhauser, Laurence A Wolsey, and Marshall L Fisher. An analysis of approximations for maximizing submodular set functions—i. *Mathematical Programming*, 14(1):265–294, 1978.
- [36] Francisco S Melo, Manuel Lopes, and Ricardo Ferreira. Analysis of inverse reinforcement learning with perturbed demonstrations. In *ECAI*, pages 349–354, 2010.
- [37] Bernard Michini, Thomas J Walsh, Ali-Akbar Agha-Mohammadi, and Jonathan P How. Bayesian nonparametric reward learning from demonstration. *IEEE Transactions on Robotics*, 31(2):369–386, 2015.

A Behavioral equivalence classes

Theorem 3. [2] Given an MDP, $BEC(\pi)$ is given by the following intersection of halfspaces:

$$\mathbf{w}^T (\mu_{\pi}^{(s,a)} - \mu_{\pi}^{(s,b)}) \geq 0, \quad (10)$$

$$\forall a \in \arg \max_{a' \in \mathcal{A}} Q^*(s, a'), b \in \mathcal{A}, s \in \mathcal{S} \quad (11)$$

$\mathbf{w} \in \mathbb{R}^k$ are the reward function weights, $\mu_{\pi}^{(s,a)} = \mathbb{E}[\sum_{t=0}^{\infty} \gamma^t \phi(s_t) | \pi, s_0 = s, a_0 = a]$, is the vector of expected feature counts from taking action a in state s and acting optimally thereafter.

Proof. In every state s we can assume that there is one or more optimal actions a . For each optimal action $a \in \arg \max_{a' \in \mathcal{A}} Q^*(s, a')$, we then have by definition that

$$Q^*(s, a) \geq Q^*(s, b), \quad \forall b \in \mathcal{A} \quad (12)$$

Rewriting this in terms of expected discounted feature counts we have

$$w^T \mu_{\pi}^{(s,a)} \geq w^T \mu_{\pi}^{(s,b)}, \quad \forall b \in \mathcal{A} \quad (13)$$

Thus, the behavioral equivalence class is the intersection of the following half-spaces

$$w^T (\mu_{\pi}^{(s,a)} - \mu_{\pi}^{(s,b)}) \geq 0, \quad (14)$$

$$\forall a \in \arg \max_{a' \in \mathcal{A}} Q^*(s, a'), b \in \mathcal{A}, s \in \mathcal{S}. \quad (15)$$

□

We can define the BEC for a set of demonstrations \mathcal{D} from a policy π similarly:

Corollary 2. $BEC(\mathcal{D}|\pi)$, is given by the following intersection of halfspaces:

$$\mathbf{w}^T (\mu_{\pi}(s, a) - \mu_{\pi}(s, b)) \geq 0, \quad \forall (s, a) \in \mathcal{D}, b \in \mathcal{A}. \quad (16)$$

Proof. The proof follows from the proof of Theorem 3 by only considering half-spaces corresponding to optimal (s, a) pairs in the demonstration. □

B Example

Given an MDP with finite states and actions, we can calculate $\text{BEC}(\pi)$ via the following result, proved by Ng and Russell [2], which is equivalent to Theorem 1.

Corollary 3. *Given a finite state space \mathcal{S} with a finite number of actions \mathcal{A} , policy π is optimal if and only if reward function R satisfies*

$$(\mathbf{T}_\pi - \mathbf{T}_a)(\mathbf{I} - \gamma\mathbf{T}_\pi)^{-1}\mathbf{R} \geq 0, \forall a \in \mathcal{A} \quad (17)$$

where \mathbf{T}_a is the transition matrix associated with always taking action a , \mathbf{T}_π is the transition matrix associated with policy π , and \mathbf{R} is the column vector of rewards for each state $s \in \mathcal{S}$.

Proof. See Ng and Russell [2]. □

Consider the grid world shown in Figure 1(a) (see the main text) with four actions (up, down, left, right) available in each state and deterministic transitions. Actions that would leave the grid boundary (such as taking the up action from the states in the top row) result in a self-transition. We computed the BEC region defined by Theorem 3:

$$(\mathbf{T}_\pi - \mathbf{T}_a)(\mathbf{I} - \gamma\mathbf{T}_\pi)^{-1}\Phi\mathbf{w} \geq 0$$

for $a \in \{\text{up, down, left, right}\}$, setting $\gamma = 0.9$ and using a featurized reward function $R(s) = w^T\phi(s)$, where $w = (w_0, w_1)$ is the binary feature weight vector with w_0 indicating “white” and w_1 indicating “shaded”. See Appendix for details. We can express the vector of state rewards as $\mathbf{R} = \Phi\mathbf{w}$, where

$$\Phi = [\phi(s_0)^T, \phi(s_1)^T, \phi(s_2)^T, \phi(s_3)^T, \phi(s_4)^T, \phi(s_5)^T]$$

and $\phi(s_i) = (1, 0)$ for $i \in \{0, 2, 3, 4, 5\}$ and $\phi(s_1) = (0, 1)$, are the feature vectors for each state numbered left to right top to bottom.

The computation results in the following non-redundant constraints that fully define $\text{BEC}(\pi)$ for π given in Figure 1:

$$2.539w_0 - w_1 \geq 0, \quad -w_0 \geq 0. \quad (18)$$

These constraints exactly describe the set of rewards that make the policy shown in Figure 1(a) optimal. This can be seen by noting that the constraints ensure that all feature weights are non-positive, because a positive weights would cause the optimal policy to avoid early termination to accumulate as much reward as possible. We also have the constraint that if we start in state 3, it is better to move down and around the shaded state then to go directly to the terminal state, this means

$$w_0 + \gamma w_0 + \gamma^2 w_0 + \gamma^3 w_0 + \gamma^4 w_0 \geq w_0 + \gamma w_1 + \gamma^2 w_0 \quad (19)$$

$$\Leftrightarrow (1 + \gamma^2 + \gamma^3)w_0 \geq w_1 \quad (20)$$

which gives us the second constraint using $\gamma = 0.9$. It is straightforward to complete similar inequalities for all states to check that $0 \geq w_0$ and $2.539w_0 \geq w_1$ are the only non-redundant constraints.

Computing the intersection of halfspaces corresponding to the demonstration gives the following convex cone

$$-w_1 \geq 0, \quad w_1 - w_2 \geq 0. \quad (21)$$

Note that the second constraint on the difference between the two feature weights is looser than the BEC region for the entire optimal policy. This is because the demonstration only shows that both features are non-positive (making the terminal a goal) and that w_2 is no better than w_1 (otherwise the demonstration would have gone through the shaded region). The demonstration leaves open the possibility that all feature weights are equal. We also note that if the demonstration had started in the top right cell, the BEC region of the demonstration would equal the BEC region of the optimal policy.

C Uncertainty Volume Minimization Algorithm

Pseudo-code for the UVM algorithm is shown in Algorithm 2.

Consider the MDP shown in Figure 5. When the UVM algorithm is run on this task the algorithm exits the while-loop reporting that the uncertainty has gone to zero and returns the demonstration set shown in Figure 6. This is clearly not an optimal demonstration since the starting state in the upper right has never been demonstrated so the agent has no idea what it should do from that state.

This highlights a problem that the UVM algorithm has with estimating volumes. If there are ever two actions that are optimal in a given state s , and those two actions (call them a and b) are demonstrated, then we will have the following halfspace constraints:

$$w^T(\mu_\pi^{(s,a)} - \mu_\pi^{(s,b)}) \geq 0 \quad (22)$$

$$w^T(\mu_\pi^{(s,b)} - \mu_\pi^{(s,a)}) \geq 0 \quad (23)$$

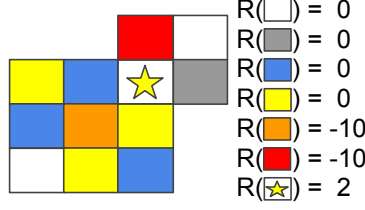


Figure 5: MDP with two initial start states.

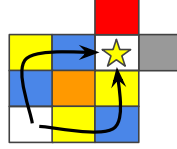


Figure 6: Demos resulting in false zero uncertainty.

Thus, we have $w^T(\mu_\pi^{(s,b)} - \mu_\pi^{(s,a)}) = 0$.

This is problematic since any strict subspace of \mathbb{R}^k has measure zero, resulting in an uncertainty volume of zero. Thus, for any optimal policy where there exists a state with two or more optimal actions, the UVM algorithm will terminate with zero uncertainty if these two optimal actions are added to \mathcal{D} . This is true, even if this leaves an entire $(k - 1)$ dimensional subspace of uncertainty over the reward.

Algorithm 2 Uncertainty Volume Minimization

Require: Set of possible initial states S_0

Require: Feature weights \mathbf{w} of the optimal reward function

- 1: Initialize $\mathcal{D} \leftarrow \emptyset$
 - 2: Compute optimal policy π^* based on \mathbf{w}
 - 3: **repeat**
 - 4: $\zeta_{\text{best}} \leftarrow \langle \rangle$
 - 5: **for all** $s_0 \in S_0$ **do**
 - 6: Generate K trajectories from s_0 following π^*
 - 7: **for** $j \in [1, K]$ **do**
 - 8: **if** $G(\mathcal{D} \cup \zeta_j) < G(\mathcal{D} \cup \zeta_{\text{best}})$ and $\zeta_j \notin \mathcal{D}$ **then**
 - 9: $\zeta_{\text{best}} \leftarrow \zeta_j$
 - 10: **end if**
 - 11: **end for**
 - 12: **end for**
 - 13: $\mathcal{D} \leftarrow \mathcal{D} \cup \zeta_{\text{best}}$
 - 14: **until** ζ_{best} **is null**
 - 15: **return** Demonstration set \mathcal{D}
-

D Removing redundant constraints

A redundant constraint is one that can be removed without changing the BEC region. We can find redundant constraints efficiently using linear programming. To check if a constraint $a^T x \leq b$ is binding we can remove that constraint and solve the linear program with $\max_x a^T x$ as the objective. If the optimal solution is still constrained to be less than or equal to b even when the constraint is removed, then the constraint can be removed. However, if the optimal value is greater than b then the constraint is non-redundant. Thus, all redundant constraints can be removed by making one pass through the constraints, where each constraint is immediately removed if redundant. We optimize this approach by first normalizing each constraint and removing duplicates and any trivial, all zero constraints.

E Set-cover algorithm termination

Proposition 2. *The set-cover machine teaching algorithm for IRL always terminates.*

Proof. To prove that our algorithm always terminates, consider the polyhedral cone $C_f = \{x \in \mathbb{R}^n \mid A_f x \geq 0\}$ that represents $\text{BEC}(\pi^*)$. Each demonstrated state action pair, (s, a) defines a set of half spaces

$$w^T(\mu(s, \pi^*(s)) - \mu(s, a)) \geq 0, \forall a \in \mathcal{A}. \quad (24)$$

When the intersection of the halfspaces for every $(s, a) \in \mathcal{D}$ is equal to $\text{BEC}(\pi^*)$, the algorithm terminates and returns \mathcal{D} . For discrete domains, $\text{BEC}(\pi^*)$ is simply the intersection of a finite number of half-spaces from every optimal (s, a) pair, so once every optimal (s, a) has been demonstrated, the algorithm is guaranteed to terminate. In practice, $\text{BEC}(\pi^*)$ can be fully defined by only a subset of the possible demonstrations. Thus, our machine teaching algorithm seeks to select the minimum number of demonstrations that cover all of the rows of A_f .

For continuous domains, we cannot fully enumerate every optimal (s, a) -pair. However, it is possible to approximate $\text{BEC}(\pi^*)$ by sampling optimal rollouts from the state space. We then solve the constraint set-cover problem using these same sampled rollouts, so we are again guaranteed to terminate once all demonstrations are chosen, and will likely terminate after only selecting a small subset of the sampled demonstrations. \square

Proposition 3. *The set-cover machine teaching algorithm is a $(1 - 1/e)$ -approximation to the minimum number of demonstrations needed to fully define $\text{BEC}(\pi^*)$.*

Proof. This result follows from the submodularity of the set cover problem [34, 35]. \square

F Optimality of set cover algorithm

We now prove the condition under which our proposed algorithm is a $(1-1/e)$ -approximation of the solution to the Machine Teaching Problem for IRL.

Both the UVM and SCOT algorithms focus on teaching halfspaces to an IRL algorithm to define the behavioral equivalence region, $\text{BEC}(\pi^*)$. Thus, they assume that when the IRL algorithm receives state-action pair (s, a) from the demonstrator, the IRL algorithm will enforce the constraint that $Q^*(s, a) \geq Q^*(s, b), \forall b \in \mathcal{A}$. We call this assumption the *halfspace assumption*.

Definition 1. *The halfspace assumption is that $Q^*(s, a) \geq Q^*(s, b), \forall b \in \mathcal{A}, (s, a) \in \mathcal{D}$.*

We now prove that, under the assumption of error-free demonstrations, three common IRL algorithms make the halfspace assumption: Bayesian IRL [24, 25], Policy Matching [26], and Maximum Likelihood IRL [8, 27].

Lemma 1. *Under the assumption of error-free demonstrations, Bayesian IRL [24, 25] makes the halfspace assumption.*

Proof. Bayesian IRL uses likelihood

$$P_{\text{opt}}(\mathcal{D}|R) = \prod_{(s,a) \in \mathcal{D}} \frac{e^{\alpha Q^*(s,a)}}{\sum_{b \in \mathcal{A}} e^{\alpha Q^*(s,b)}} \quad (25)$$

where Q^* is the optimal Q -function under reward function R and $\alpha \in [0, \infty)$ represents the confidence that the demonstrations come from π^* . As $\alpha \rightarrow \infty$, Bayesian IRL assume error-free demonstrations and we have

$$\lim_{\alpha \rightarrow \infty} P_{\text{opt}}(\mathcal{D}|R) = 0 \iff \exists b \in \mathcal{A}, \text{ s.t. } Q^*(s, a) < Q^*(s, b). \quad (26)$$

Thus, Bayesian IRL only gives positive likelihood to reward functions R , if $Q^*(s, a) \geq Q^*(s, b) \forall b \in \mathcal{A}, (s, a) \in \mathcal{D}$. \square

Corollary 4. *Under the assumption of error-free demonstrations, Policy Matching [26] makes the optimal teaching assumption.*

Proof. Melo et al. [36] proved that Bayesian IRL [24] and Policy Matching [26] share the same reward solution space. Thus, the lemma follows from the previous proof. \square

Corollary 5. *Under the assumption of error-free demonstrations, Maximum Likelihood IRL [8, 27] makes the optimal teaching assumption.*

Proof. Maximum Likelihood IRL uses the same likelihood function as Bayesian IRL, thus the result follows from the previous lemma. \square

Table 2: Comparison of different optimal teaching algorithms across random 9x9 grid worlds with 8-dimensional binary features. Algorithms compared are Uncertainty Volume Minimization (UVM), Set Cover Optimal Teaching (SCOT) with and without redundancies, and random sampling from the optimal policy. UVM(x) was run using x Monte Carlo samples for volume estimation. Results show the average number of state-action pairs in the demonstration set \mathcal{D} , the average number of suboptimal actions when performing IRL using \mathcal{D} learned policy compared to optimal, and the average run time of the optimal teaching algorithm in seconds. All results are averaged over 20 replicates.

	Ave. (s, a) pairs	Ave. % incorrect actions	Ave. time (s)
UVM (10^4)	3.850	44.074	247.944
UVM (10^5)	5.150	31.420	567.961
UVM (10^6)	6.650	19.568	1620.578
UVM (10^7)	8.450	18.642	10291.365
SCOT (redundant)	66.250	0.494	9.858
SCOT	16.200	0.679	0.901
Random	20.0	10.556	0.000

We can now prove the following Theorem:

Theorem 4. *Under the assumption of error-free demonstrations, SCOT is a $(1 - 1/e)$ -approximation to the Machine Teaching Problem for IRL (Section 3.3) for the following learning algorithms:*

- *Bayesian Inverse Reinforcement Learning [24, 25]*
- *Policy Matching [26]*
- *Maximum Likelihood Inverse Reinforcement Learning [8, 27]*

Proof. Given an IRL algorithm that makes the halfspace assumption, by Proposition 3 SCOT will find a set of demonstrations that are a $(1-1/e)$ -approximation of the maximally informative demonstration set. Thus, by Lemma 1, in the limit as $\alpha \rightarrow \infty$, the SCOT machine teaching algorithm is a $(1-1/e)$ -approximation to the optimal demonstration set for Bayesian IRL. Similarly, by corollaries 4 and 5, SCOT is a $(1-1/e)$ -approximation to the optimal demonstration set for Policy Matching and Maximum Likelihood IRL. \square

G Algorithm comparison full results

We compared the SCOT algorithm with the UVM algorithm of Cakmak and Lopes [13]. We also report here a comparison against SCOT without removing redundancies and against random selected demonstrations from the optimal policy.

We ran an experiment on random 9x9 grid worlds with 8 binary indicator features per cell with one feature active per cell and $\gamma = 0.95$. For this experiment the demonstrations were single state-action pairs. We measured the 0-1 policy loss [37] for each demonstration set by computing the percentage of states where the resulting policy took a suboptimal action under the true reward. The policy was found by first finding the maximum likelihood reward function [8, 27], by using BIRL [24] with a uniform prior and $\alpha = 100$. We ran the MCMC chain for 10,000 steps using $\alpha = 100$ and step size of 0.005. Given the maximum likelihood reward function, the corresponding policy was then found using value iteration. The results are shown in Table 2.

We found that the UVM algorithm usually underestimates the size of the optimal teaching set of demonstrations, due to the difficulty of estimating volumes as discussed earlier, resulting in high 0-1 loss. We tried sampling more points, but found that this only slightly improved 0-1 loss while significantly increasing run-time. Compared to UVM, our results show that SCOT is more accurate and more efficient—it can successfully find good demonstrations that lead to IRL learning the correct reward and corresponding policy, with orders of magnitude less computation time. We also found that removing redundant halfspaces is important; keeping redundant constraints results in slightly lower average performance loss, due to the randomness in MCMC, but finds demonstration sets that are much larger. SCOT removes redundant half-space constraints which results in solutions with fewer state-action pairs and a faster run-time, since the set-cover problem is substantially reduced in size.

We also compared against randomly sampling 20 state-action pairs from the optimal policy. The results show that SCOT is able to find informative demonstrations that significantly reduce the number of (s, a) pairs to teach a policy, compared to sampling i.i.d. from the policy.

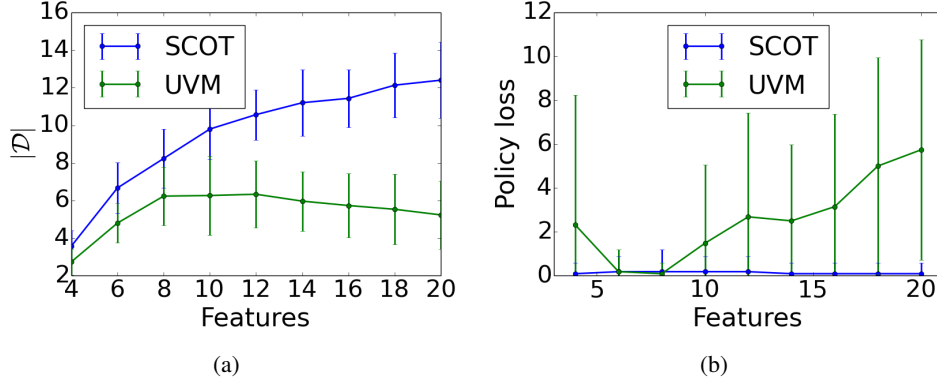


Figure 7: SCOT algorithm is robust to increasing numbers of features, whereas UVM is not robust since it relies on good volume estimates. Results averaged over 30 runs on a 6x6 grid world. UVM uses 1,000,000 samples for volume estimation.

To further explore the sensitivity of UVM to the number of features, we ran a test on a fixed 6x6 size grid world with varying numbers of features. We wanted to see if using UVM and SCOT to teach a deterministic policy would avoid the early stopping problem for UVM by avoiding the problem of having multiple optimal actions from the same starting position. We also investigated using longer demonstrations with a horizon of 6. We found that the SCOT algorithm picks more demonstrations as the number of features increases, however, the UVM algorithm cannot reliably estimate volumes for higher-dimensional spaces. The results are shown in Figure 7. The number of state-action pairs in the demonstrations are shown to plateau and even slightly decrease for UVM. Thus, UVM underestimates the number of required demonstrations to teach an optimal policy for high-dimensional features while still requiring nearly three orders of magnitude more computation time.

H Active learning experiment parameters

We generated 10x10 random grid worlds where each state was assigned a random one-hot 10-dimensional feature vector we set the discount factor to $\gamma = 0.95$. We ran BIRL with a uniform prior to obtain the MAP reward function given demonstrations for each active IRL algorithm. Each active query resulted in an optimal trajectory of length 20 demonstrated from the optimal policy. We ran the MCMC chain for 10,000 steps using $\alpha = 100$ and step size of 0.005.

I BIO-IRL algorithm specifics

We calculate angular similarity as follows: We take all the normal vectors from $\text{BEC}(D|\pi^*)$ and do a greedy matching to $\text{BEC}(\pi^*)$. Since the normal vectors are unit vectors we simply compute the dot product as similarity and once we match the first vector in $\text{BEC}(D|\pi^*)$ with the closest vector in $\text{BEC}(\pi^*)$, we remove the best match from $\text{BEC}(\pi^*)$ and continue with the next vector in $\text{BEC}(D|\pi^*)$. When there are no remaining halfspaces in $\text{BEC}(D|\pi^*)$ The algorithm returns the cumulative sum of angular similarities divided by the number of halfspaces in $\text{BEC}(\pi^*)$.

Because our normal vectors can have positive and negative elements, we use the angular similarity defined as

$$\text{AngularSim}(x_1, x_2) = 1 - \cos^{-1}(x_1 \cdot x_2) / \pi \quad (27)$$

to measure the similarity between two halfspaces.

I.1 Markov chain BIO-IRL experiment

We used $\alpha = 100$ as the softmax temperature parameter for BIRL and BIO-IRL.

I.2 Ball sorting BIO-IRL experiment

We discretized the table top into a 6x6 grid of positions, all of which are potential starting states. The four discrete actions move the ball along the table top in the four cardinal directions. The demonstrations consisted of optimal trajectories found using Value Iteration of length 10. BIRL and BIO-IRL both used the following parameters: $\alpha = 100$, MCMC chain length=1000, MCMC step size = 0.05. BIO-IRL used $\lambda = 100$.